

## The 14 $\mu\text{m}$ Band of Carbon Stars<sup>0</sup>

I. Yamamura, T. de Jong<sup>1</sup>, L.B.F.M. Waters<sup>2</sup>, J. Cami<sup>2</sup>

*Astronomical Institute 'Anton Pannekoek', University of Amsterdam,  
Kruislaan 403, 1098 SJ, the Netherlands*

K. Justtanont

*Stockholm Observatory, 13336 Saltsjöbaden, Sweden*

**Abstract.** We have studied the absorption bands around 14  $\mu\text{m}$  in the spectra of 11 carbon stars with mass-loss rates ranging from  $10^{-8}$  to  $10^{-4}$   $M_{\odot} \text{yr}^{-1}$ , based on data obtained with the Short Wavelength Spectrometer (SWS) on board the Infrared Space Observatory (ISO). All stars clearly show a  $\text{C}_2\text{H}_2$  absorption band peaking at 13.7  $\mu\text{m}$ , while the contribution from HCN molecules is small in this wavelength region. A simple plane-parallel LTE model with two layers at different temperatures is used to derive the  $\text{C}_2\text{H}_2$  abundances in the outer photosphere and in the circumstellar envelope. We find that (1) the column density of the hot-layer, placed at about  $3R_{\star}$  with a temperature of 1400 K is roughly the same for all stars regardless of the mass-loss rate, and (2) the contribution of cool molecules in the circumstellar envelope increases with the dust mass-loss rate, (3) the abundance of  $\text{C}_2\text{H}_2$  in the two layers is about the same, i.e. no obvious depletion of  $\text{C}_2\text{H}_2$  molecules seems to occur in the circumstellar envelope.

### 1. Introduction

Acetylene ( $\text{C}_2\text{H}_2$ ) is the most abundant molecule in the atmosphere of carbon stars after CO and HCN (Tsuji 1964). The molecule probably plays an essential role in the atmosphere of these stars, not only in the energy budget through their ro-vibrational transitions but also as a seed molecule for dust formation.  $\text{C}_2\text{H}_2$  has been little studied, however, since the linear and symmetric structure of  $\text{C}_2\text{H}_2$  prevents us to observe the molecule directly at radio frequencies. The abundance of the molecule has been estimated from its photodissociation products such as  $\text{C}_2\text{H}$  (Keady & Hinkle 1988, Fuente et al. 1998). The ro-vibrational

---

<sup>0</sup>Based on observations with ISO, and ESA project with instruments funded by ESA Member States (especially the PI countries: France, Germany, the Netherlands and the United Kingdom) with the participation of ISAS and NASA. The SWS is a joint project of SRON and MPE.

<sup>1</sup>also SRON-Utrecht, Sorbonnelaan 2, 3584 CA, Utrecht, the Netherlands

<sup>2</sup>also SRON-Groningen, Landleven 12, 9700 AV, Groningen, the Netherlands

transitions in the infrared are also not easy to measure. The  $3.05\ \mu\text{m}$  absorption band is accessible from the ground, but very high resolution is required in order to avoid confusion with other molecules such as HCN. The band centers of other major transitions at  $7.5$  and  $13.7\ \mu\text{m}$  are inaccessible from the ground, and have only been partially observed (Keady & Ridgway 1993).

The ISO/SWS (Kessler et al. 1996, de Graauw et al. 1996) provides infrared spectra in a broad wavelength range with moderately high resolution. As a part of the ISO guaranteed time program AGBSTAR, we observed 11 carbon stars with various mass-loss rates ranging from  $10^{-8}$  and  $10^{-4}\ \text{M}_{\odot}\ \text{yr}^{-1}$ . Based on the infrared spectra of these stars we concluded that not only the energy distribution and the broad dust features but also several narrow molecular features drastically change with the mass-loss rate (Yamamura et al. 1998). In this article, we focus on the  $\text{C}_2\text{H}_2$  band at  $13.7\ \mu\text{m}$ , and discuss the  $\text{C}_2\text{H}_2$  distribution around the stars. This band has sharp Q-branch, which makes it easier to identify and distinguish it from other molecular features.

## 2. Observations and results

The observations were carried out using the SWS AOT01 full-grating scan mode. All stars were observed with a resolution of about 300, except IRC+10216 which was observed at a resolution of about 1000. The data were reduced by the SWS Interactive Analysis package developed by the SWS instrument dedicated team, using the most recent set of calibration parameters (as of April 1998).

The carbon star sample is divided into four groups (II–V) based on their near-infrared color temperature,  $T_{\text{NIR}}$ , which is supposed to be a good indicator of mass-loss rate (Groenewegen et al. 1992). The spectra of our carbon stars between  $13$  and  $15\ \mu\text{m}$  are shown in Figure 1, labeled with their name and group number. The spectra are normalized to the *local continuum*. The spectra are also shifted slightly with respect to the model spectra in order to correct for the ambiguity in the absolute continuum level. The uncertainty in the continuum determination will be discussed in Section 4.1.

The  $\text{C}_2\text{H}_2$  band at  $13.7\ \mu\text{m}$  is clearly detected in *absorption* in all stars, regardless of the mass-loss rate. The band is actually a mixture of many Q-branches including the  $\nu_5$  fundamental transition. The band is broader in stars with smaller mass-loss rate, indicating that the absorption is due to hot gas near the photosphere. On the other hand, the HCN band at  $14.0\ \mu\text{m}$  is hardly recognized in any of the spectra in Figure 1. Indeed, the feature is much weaker than that expected from the far-infrared spectrum of IRC+10216 (Cernicharo et al. 1996) or from the  $3.6\ \mu\text{m}$  feature in the same SWS spectra. This may be explained in terms of the distribution of the molecule as well as the excitation mechanism, but it is the subject for future studies.

The spectra are in contrast with those of oxygen-rich stars, which exhibit  $\text{CO}_2$  emission bands in the same wavelength range (Justtanont et al. 1998, Cami et al. 1997). This indicates that there is always a continuum source behind the  $\text{C}_2\text{H}_2$  molecule.

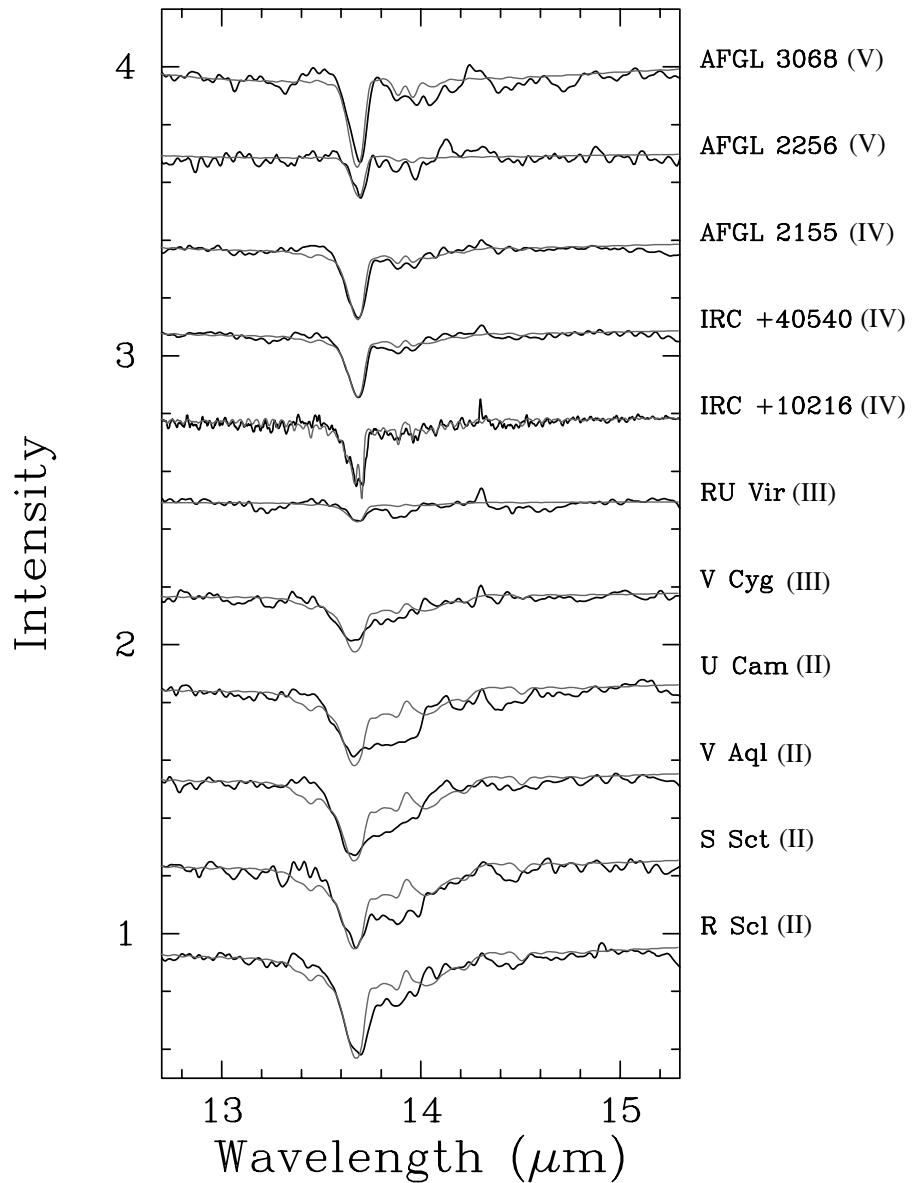


Figure 1. The  $14 \mu\text{m}$  band of carbon stars (*solid line*) is shown with the model spectra (*gray line*). The spectra are ordered by decreasing near-infrared color temperature ( $T_{\text{NIR}}$ ) from bottom to top. The group number of each object is indicated after the object name. The spectra are normalized to the *local continuum*. In addition, they are shifted within 7 % when compared with the models, in order to correct for the uncertainty in the absolute continuum levels. The fit is not so good for group II stars especially between  $13.8$  and  $14.0 \mu\text{m}$  due to insufficient molecular line data.

### 3. Modeling

Quantitative analysis of the spectra is attempted with a simple plane-parallel model. In order to simplify the problem as much as possible, we try to explain the observed spectra by combination of two components: a *hot-component* representing photosphere and a *cool-component* corresponding to the circumstellar envelope. Each layer is characterized by three parameters, the column density ( $N$ ), the excitation temperature ( $T$ ), and the turbulent velocity ( $v_{\text{turb}}$ ). In the present calculation,  $v_{\text{turb}}$  is fixed as  $3 \text{ km s}^{-1}$  in both layers. The results are insensitive to the value of  $v_{\text{turb}}$ . For instance, for  $v_{\text{turb}} = 10 \text{ km s}^{-1}$  the column density would only decrease by 0.1 dex. Only  $\text{C}_2\text{H}_2$  is considered. The line data are based on Kabbadj et al. (1991), Rinsland et al. (1982), Palmer et al. (1972), and Weber et al. (1994). About 20000 lines are included in the wavelength region in Figure 1. From a comparison with laboratory spectra (Kawaguchi, private communication), it is known that the line data are incomplete, especially between  $13.8$  and  $14.0 \mu\text{m}$ . We ignored that part in the fitting.

First, the temperatures of the two layers are determined. We assume that group II and group V stars represent the hot- and cool-component, respectively, and we fit their spectra by a single layer model. For every combination in the parameter space of  $10^{15} \leq N \leq 10^{19} \text{ cm}^{-2}$  with 0.1 dex step and  $300 \leq T \leq 1800 \text{ K}$  with 50 K interval, the model spectrum is characterized by the *rms* of the residual from the observed spectrum, and the best fit is the one which minimizes the *rms*. We obtain  $T_{\text{hot}} = 1400 \text{ K}$  and  $T_{\text{cool}} = 450 \text{ K}$ . In the second step, we fix the temperatures at these values and fit all stars with two layers model by the same procedure in  $(N_{\text{hot}}, N_{\text{cool}})$  space. The best fit spectra are shown in Figure 2 by gray lines, and the derived column densities for the spectra are plotted in Figure 2 as a function of  $T_{\text{NIR}}$ .

The emission from the dust envelope fills in and weakens the absorption in the photosphere. The correction of this effect is attempted as follows: A model spectrum with  $N_{\text{hot}}$  and  $T_{\text{hot}}$  is calculated. The spectrum is then surrounded by a spherical dust envelope model with a certain mass-loss rate, and a synthesized spectrum is calculated. A star with a blackbody temperature of  $2500 \text{ K}$  and radius  $3 \times 10^{13} \text{ cm}$  is used when the dust temperature distribution is calculated. The envelope is assumed to extend from  $10 R_{\star}$  to  $10^4 R_{\star}$ . The weakened molecular feature in the output spectrum may have an intensity similar to that with a lower column density and no dust effect. The difference between the original and weakened spectrum in terms of the column density is the correction factor corresponding to the dust mass-loss rate. The dust mass-loss rate of each star is determined by adopting the same model to their SWS spectra. The corrected values of  $N_{\text{hot}}$  are also plotted in Figure 2.

### 4. Discussion

#### 4.1. Uncertainty in the result

$\text{C}_2\text{H}_2$  molecules can be as abundant as  $10^{-4}$  in the photosphere when the temperature is below about  $2000 \text{ K}$  (Tsuji 1964). We find that when the column density exceeds about  $10^{19} \text{ cm}^{-2}$  and the temperature is high, the sharp feature at  $13.7 \mu\text{m}$  disappears and the  $\text{C}_2\text{H}_2$  band becomes rather smooth, deep absorp-

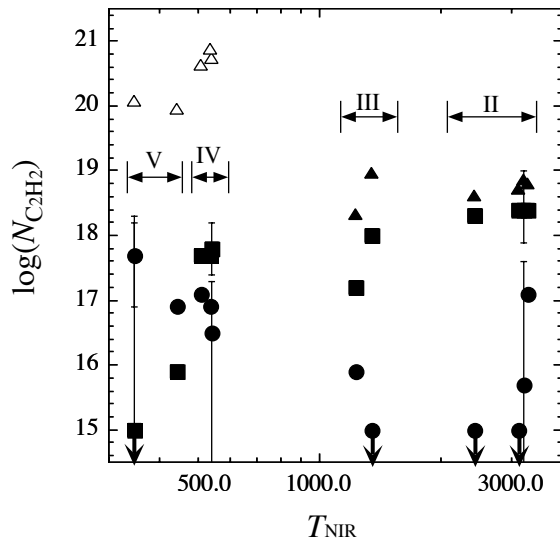


Figure 2. The column densities of  $C_2H_2$  molecules in hot (*squares*) and cool (*circles*) layers are plotted against the near-infrared temperature. The hot-layer column densities after correction for dust emission effect are also plotted (*triangle*). The correction may be proper only for the low mass-loss rate stars (*filled triangles*). The error bars given in some data indicate the approximate uncertainty of the results in general. Symbols with arrows are upperlimits.

tion from  $10 \mu\text{m}$  to over  $20 \mu\text{m}$  due to heavy saturation effects. Presumably, the *continuum* we draw in the present analysis is actually this continuous absorption, and the features we call *hot-component* is a layer just above this hottest, innermost part of the atmosphere.

The dust envelope also affects the results of the cool layer. Especially when the envelope has a moderate optical depth, the present plane parallel model potentially underestimates the column density of the cool layer, since it does not consider the size difference between two layers. This effect is small even in the most optically thick envelopes (group V), in which the circumstellar dust emission is the only continuum source.

#### 4.2. Column densities of two layers

The column density in the hot-layer is almost constant at  $10^{18.7} \text{ cm}^{-2}$  in group II and III stars. The value increases considerably in groups IV and V, but this may be an artifact because the dust mass-loss rate of these stars is too high to be able to apply this correction method and may have large uncertainties.

$N_{\text{cool}}$  increases as  $T_{\text{NIR}}$  decreases. Since  $T_{\text{NIR}}$  refers the dust mass-loss rate of the stars, the good correlation between two quantities indicates that the  $C_2H_2$  molecule is associated with the dust envelope. One interesting exception is R Scl, which shows a significant  $N_{\text{cool}}$  although its  $T_{\text{NIR}}$  is the highest in the sample. This star is known to have a rather thick, probably detached circumstellar shell (Oloffson et al. 1990) and a relation between cool  $C_2H_2$  and such an envelope is probable.

### 4.3. C<sub>2</sub>H<sub>2</sub> abundance

Despite the uncertainties described above, it is still worth to make estimates of the abundance of C<sub>2</sub>H<sub>2</sub> in the two layers. According to the dynamic model atmosphere by Höfner & Dorfi (1997), the temperature of the hot layer, 1400 K, can be achieved at the distance of about  $3 R_*$  from the central star. The density of the region is about  $3 \times 10^9 \text{ H}_2 \text{ cm}^{-3}$ . Assuming that the molecule is distributed between the surface ( $1 R_*$ ) and  $3 R_*$ , the column density  $10^{18.7} \text{ cm}^{-2}$  is converted to an abundance of  $2 \times 10^{-5}$ . In the circumstellar envelope, we assume that the density decreases proportionally to the square of radius. We take AFGL 3068 as an example. The expansion velocity and the mass-loss rate measured by CO observations is  $14 \text{ km s}^{-1}$  and  $2 \times 10^{-5} M_\odot \text{ yr}^{-1}$  (Loup et al. 1993), and the column density derived by the model analysis is  $10^{17.7} \text{ cm}^{-2}$ . Assuming the inner radius of the envelope as  $3 \times 10^{14} \text{ cm}$ , we obtain  $7 \times 10^{-6}$ .

These values are in good agreement with previous estimates of the C<sub>2</sub>H<sub>2</sub> abundance (e.g., Keady & Hinkle 1988, Fuente et al. 1998). Our results indicate that the abundance does not change drastically in the regions below and above the dust forming region. i.e., no significant depletion of C<sub>2</sub>H<sub>2</sub> onto grains seems to take place at the dust forming region.

**Acknowledgments.** The authors are grateful to Prof. K. Kawaguchi for providing the laboratory spectra of C<sub>2</sub>H<sub>2</sub>. I.Y. and L.B.F.M.W. acknowledge financial support from a NWO PIONIER grant.

### References

- Cami, J., Justtanont, K., de Jong, T., et al, 1997, Proc. First ISO Workshop on Analytical Spectroscopy, A.M. Heras et al. (eds.), ESA SP-419, 159  
Cernicharo, J., Barlow, M.J., González-Alfonso, E., et al., 1996, A&A 315, L201  
de Graauw, Th., Haser, L.N., Beintema, D.A., et al. 1996, A&A 315, L49  
Fuente, A., Cernichar., J., Omont, A., 1998, A&A 330, 232  
Groenewegen, M.A.T., de Jong, T., van der Blik, N.S., Slijkhuis, S., Willems, F.J., 1992, A&A 253, 150  
Höfner, S., Dorfi, E.A., 1997, A&A 319, 648  
Justtanont, K., Feuchtgruber, H., de Jong, T., et al., 1998, A&A 330, L17  
Kabbadj, Y., Herman, M., Di Lonardo, et al., 1991, J.Mol.Spec. 150, 535  
Keady, J.J., Hinkle, K.H., 1988, ApJ 331, 539  
Keady, J.J., Ridgway, S.T., 1993, ApJ 406, 199  
Kessler, M., Steinz, J.A., Anderegg, M.E., et al. 1996, A&A 315, L27  
Loup, C., Forveille, T., Omont, A., Paul, J.F., 1993, A&AS 99, 291  
Olofsson, H., Carlström, Eriksson, K., et al., 1990, A&A 230, L13  
Palmer, K.F., Mickelson, M.E., Rao, K.N., 1972, J.Mol.Spec. 44, 131  
Rinsland, C.P., Baldacci, A., Rao, K.N., 1982, ApJS 49, 487  
Tsuji, T., 1964, Ann.Tokyo Astr.Obs. 2nd.Ser 9, 1  
Weber, M., Blass., W.E., Halsey, G.W., et al., 1994, J.Mol.Spec. 165, 107  
Yamamura, I., de Jong, T., Justtanont, K., et al., 1998, Ap&SS 255, 351